Free Radical Biology and Medicine 126 (2018) 322–333

Contents lists available at ScienceDirect

Free Radical Biology and Medicine

journal homepage: www.elsevier.com/locate/freeradbiomed

Original article

Altered cellular redox homeostasis and redox responses under standard oxygen cell culture conditions *versus* physioxia

Daniel C.J. Ferguson[a], Gary R. Smerdon[a,b], Lorna W. Harries[a], Nicholas J.F. Dodd[c], Michael P. Murphy[d], Alison Curnow[e], Paul G. Winyard[a,*]

[a] University of Exeter Medical School, Exeter, Devon EX1 2LU, UK
[b] DDRC Healthcare, Plymouth Science Park, Research Way, Plymouth, Devon PL6 8BU, UK
[c] University of Plymouth, Drake Circus, Plymouth, Devon PL4 8AA, UK
[d] MRC Mitochondrial Biology Unit, University of Cambridge, Wellcome Trust/MRC Building, Cambridge Biomedical Campus, Hills Road, Cambridge CB2 0XY, UK
[e] University of Exeter Medical School, Truro, Cornwall TR1 3HD, UK

A B S T R A C T

In vivo, mammalian cells reside in an environment of 0.5–10% O_2 (depending on the tissue location within the body), whilst standard *in vitro* cell culture is carried out under room air. Little is known about the effects of this hyperoxic environment on treatment-induced oxidative stress, relative to a physiological oxygen environment. In the present study we investigated the effects of long-term culture under hyperoxia (air) on photodynamic treatment. Upon photodynamic irradiation, cells which had been cultured long-term under hyperoxia generated higher concentrations of mitochondrial reactive oxygen species, compared with cells in a physioxic (2% O_2) environment. However, there was no significant difference in viability between hyperoxic and physioxic cells. The expression of genes encoding key redox homeostasis proteins and the activity of key antioxidant enzymes was significantly higher after the long-term culture of hyperoxic cells compared with physioxic cells. The induction of antioxidant genes and increased antioxidant enzyme activity appear to contribute to the development of a phenotype that is resistant to oxidative stress-induced cellular damage and death when using standard cell culture conditions. The results from experiments using selective inhibitors suggested that the thioredoxin antioxidant system contributes to this phenotype. To avoid artefactual results, *in vitro* cellular responses should be studied in mammalian cells that have been cultured under physioxia. This investigation provides new insights into the effects of physioxic cell culture on a model of a clinically relevant photodynamic treatment and the associated cellular pathways.

1. Introduction

The culture of primary and immortalized mammalian cells is widely employed to identify novel treatment targets for human disease and to establish the bioactivities of novel compounds during the early stages of drug development, prior to experimentation *in vivo*. Mammalian cell culture is normally carried out under humidified air supplemented with 5% CO_2, resulting in an environment containing approximately 18.6% O_2 [1,2]. In contrast, most cells in healthy human tissues reside in an environment of physiological O_2 (physioxia) ranging from about 0.5–10% (with clear exceptions, such as the lung epithelium) depending on location and proximity to the vasculature [3]. Despite this, *in vitro* investigations of cellular responses to biological stresses or therapeutic compounds give limited consideration to the effects of the long-term culture of cells in a hyperoxic environment. Consideration of such effects is important when attempting to extrapolate from *in vitro* findings to models of health and disease *in vivo*.

There is extensive literature on the effects of O_2 concentration on the efficacy of drug and radiation treatments in cancer cell killing, both *in vivo* and *in vitro* [4–9]. However, most studies have characterized these effects *in vitro* in cells that have been cultured, long-term, in a hyperoxic environment (*i.e.* air) with subsequent short-term exposure to different O_2 concentrations during various treatments (drugs, photodynamic irradiation, hypoxia-reperfusion, *etc.)* [4,5,7,9–12]. The consequences of long-term exposure to hyperoxic or physioxic environments on the subsequent cell killing effects of cancer treatments (*e.g.* gamma irradiation or photodynamic therapy), are still poorly defined.

Protoporphyrin IX (PpIX)-based photodynamic therapy is a common clinical treatment for non-melanoma skin cancers and precancers [13] which uses the natural photosensitive properties of PpIX to induce oxidative stress in targeted skin cells when activated by irradiation with red light (λ_{max} 635 nm) [14]. Non-melanoma skin cancers are the most common form of cancers diagnosed annually in the western world and, despite low mortality, the associated high morbidity [15] provides a significant incentive to identify improved, cosmetically acceptable treatments. Previous studies have considered the effects of hypoxia on the outcome of photodynamic therapies [5,16], although these were limited in their scope and did not attempt to recapitulate the O_2

* Corresponding author.
E-mail address: p.g.winyard@exeter.ac.uk (P.G. Winyard).

https://doi.org/10.1016/j.freeradbiomed.2018.08.025
Received 22 July 2018; Accepted 20 August 2018
Available online 22 August 2018
0891-5849/

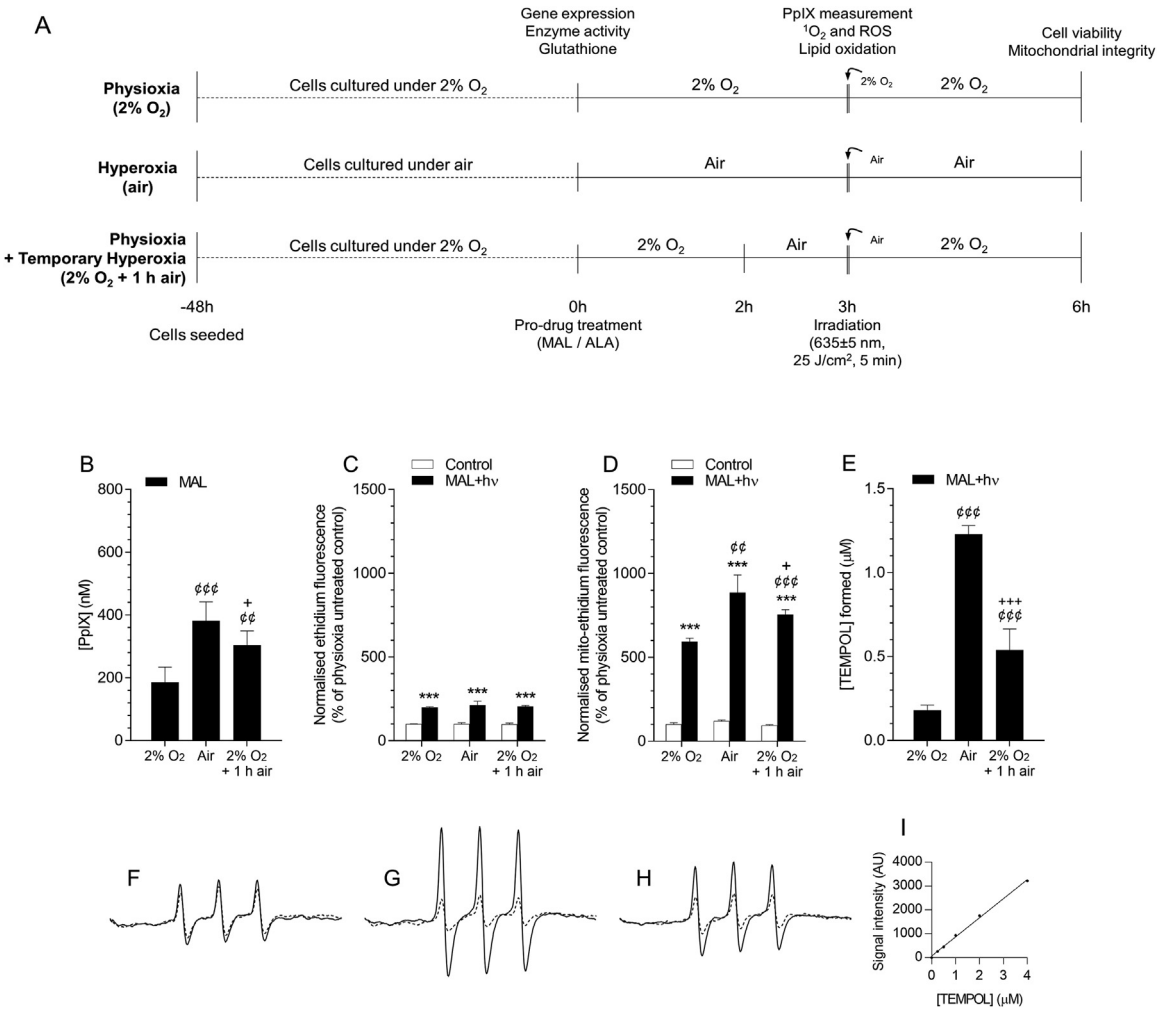

Fig. 1. The effects of physioxia and hyperoxia on MAL-induced PpIX accumulation and photo-generated reactive oxygen species in A431 cells. (A) A431 cells were subjected to different treatment protocols under conditions of "physioxia" (2% O_2), "hyperoxia" (air) or "physioxia + temporary hyperoxia" (2% O_2 + 1 h air). Arrows indicate the O_2 concentration during irradiation. (B) Protoporphyrin IX (PpIX) accumulation was measured following treatment (3 h) with 1 mM MAL under each O_2 condition (n = 6). PpIX fluorescence in treated cells was corrected by subtracting each condition's corresponding untreated (control) fluorescence. (C-E) Photo-generated ROS were detected by (C) DHE or (D) mito-DHE in conjunction with flow cytometry analysis (n = 4). and (E) electron paramagnetic resonance spectrometry (EPR). In (C) and (D), a group of cells within each O_2 condition remained untreated ("control"), i.e. no pro-drug (MAL) addition nor photoirradiation. (F-H) Pre-irradiation (dotted) and post-irradiation (solid) EPR spectra acquired from lysates of cells treated with MAL under (F) physioxia, (G) hyperoxia or (H) physioxia + temporary hyperoxia (n = 5). (I) Typical standard curve obtained by plotting TEMPOL concentration against the area of the acquired spectra. TEMPOL formed in (F), (G) and (H) was interpolated using the standard curve (I).The pre-irradiation (background) TEMPOL signal was subtracted from the post-irradiation TEMPOL signal to obtain the values displayed in (E). *** = $P < 0.001$, compared to controls. ¢¢ = $P < 0.01$, ¢¢¢ = $P < 0.001$, compared to the same treatment under "physioxia". + = $P < 0.05$, + + + = $P < 0.001$, compared to the same treatment under "hyperoxia". Data are presented as mean ± one standard deviation, with statistical significance determined by a two-tailed Student's *t*-test.

environment in which superficial epidermoid carcinomas reside. The use of a physiologically accurate *in vitro* model would therefore support the successful translation of experimental findings into *in vivo* investigations. Here, we studied the effects of culturing epidermoid carcinoma (A431) cells, for 48 hours, in a physioxic O_2 environment on the basal redox defences and subsequent oxidative stress-induced cell death (*i.e.* PpIX-based photodynamic cell killing), compared to cells cultured under standard laboratory incubator conditions (*i.e.* air). Two percent O_2 was chosen to represent a physioxic environment as this concentration falls within the range of O_2 concentrations measured in healthy epidermal skin [17] and superficial epidermoid carcinomas *in vivo* [18]. Thus, our investigations were carried out under three different O_2 conditions (Fig. 1A): (1) "physioxia", where cells were cultured and treated under 2% O_2; (2) "hyperoxia", where cells were cultured and treated under air (18.6% O_2); and (3) "physioxia + temporary hyperoxia", where cells were cultured under 2% O_2 and transiently exposed to air during treatment. This latter condition was included in an attempt to recapitulate observations made *in vivo* [8,19], where increased O_2 significantly improved photodynamic treatment efficacy. Thus, we investigated whether epidermoid carcinoma cells chronically cultured under the standard hyperoxic (18.6% O_2) cell culture conditions were less susceptible to oxidative stress-induced cell death, compared to those cultured under physioxia (2% O_2).

2. Methods

2.1. Culture of cells under different O_2 conditions

A431 human epidermoid carcinoma cells were obtained from the European Collection of Cell Cultures and cultured in Dulbecco's modified eagle's medium (DMEM; Lonza) supplemented with 10% foetal bovine serum (Lonza), 2% L-glutamine (Sigma-Aldrich) and 2% penicillin-streptomycin (pen/strep; Sigma-Aldrich). Normal human epidermal keratinocytes (NHEK) were also obtained from the European

Collection of Cell Cultures and cultured in serum-free keratinocyte medium (KGM-2; Lonza), supplemented with bovine pituitary extract, human epidermal growth factor, recombinant human insulin, hydrocortisone, epinephrine, transferrin and GA-1000 (gentamicin and amphotericin-B). The media remained unmodified for experiments on A431 and NHEK cells. Routine passaging of cells was carried out under aseptic conditions in a class II laminar flow hood approximately every 3-4 days where apprpriate and cells were incubated at 37 °C in a 5% CO_2 humidified incubator.

To culture cells under an atmosphere of any desired gas mixture, we implemented a technique like that which has been reported previously [20,21]. Airtight containers (Fig. S1) were modified with inlet and outlet pipelines with midline valves, providing a means by which a gas cylinder could be attached. Opening of the cylinder and midline valves resulted in the pre-mixed gas replacing the atmospheric air within the container. The O_2 concentration present in evacuated gas was monitored until the desired O_2 concentration was achieved. Closure of both midline valves produced a gas-tight environment and the container was then placed in a regular incubator at 37 °C. To ensure the internal environment was maintained over prolonged periods, the rubberized seals on the lid were greased (MolyKote 1102 grease; Dow Corning). For the purposes of this study, a gas mixture of 2% O_2, 5% CO_2 and 93% N_2 was made up in 10 L, 150 bar cylinders (DDRC Healthcare). Pre-gassed cell culture medium for culturing and treating cells was prepared by bubbling the medium with pre-mixed gas for at least 20 min. To minimise contact with room air, any treatment of cells cultured under physioxia was carried out within 15 s.

2.2. Measurement of O_2 within culture medium

A Free Radical Analyser (TBR4100; World Precision Instruments) was used, coupled with an O_2 electrode (ISO-OXY-2, World Precision Instruments) to measure the O_2 concentration within the culture medium (Fig. S2). A 3-point calibration was carried out using solutions equilibrated with 0% (pure N_2), 20% and 100% O_2. A standard curve was created by plotting these O_2 concentrations against the measured voltages, allowing O_2 concentrations in the culture media to be determined by interpolating the measured voltages. The O_2 electrode was placed directly into the medium and a reading was taken once the signal had stabilised (~ 10 s). This was carried out at the beginning of culture (0 h), after a day of incubation (24 h) prior to replacing the medium, and prior to experimentation (48 h).

2.3. PpIX accumulation and measurement

Intracellular accumulation of PpIX *via* the haem biosynthesis pathway was induced by treatment with the pro-drugs methyl-aminolaevulinate (MAL; 1 mM) or aminolaevulinic acid (ALA; 0.5 mM) purchased from Sigma-Aldrich. Both ALA and MAL have been used in this study as they represent the two commercially available and clinically approved pro-drugs in use in the U.S. and Europe, respectively. Working concentrations were chosen to obtain an optimal yield of PpIX from each pro-drug (data not shown). PpIX fluorescence measurements were carried out using a modified version of a previously described method [14]. Clear-bottomed, black, 96-well plates (Greiner) were seeded with A431 or NHEK cells at a density of 1.5×10^5 cells per ml (200 µl, 3×10^4 cells) and incubated under physioxia (2% O_2) or hyperoxia (air) for 48 h at 37 °C. Following incubation, cells were treated with MAL or ALA and incubated under physioxia or hyperoxia for 3 h at 37 °C. For the "physioxia + temporary hyperoxia" condition, cells were cultured and treated under physioxia (2% O_2) and subsequently exposed to hyperoxia (air) for the final 1 h of treatment prior to PpIX measurement (see Fig. 1A). Following treatment, all wells were washed with PBS, before 100 µl of PBS was pipetted into each well for the fluorescence measurement. An 8-point standard curve of pre-synthesized PpIX (0–2 µM) was prepared for later interpolation of intracellular PpIX concentrations. Fluorescence was measured using a BMG Labtech Pherastar plate reader (excitation 410 nm, emission 630 nm).

2.4. Photodynamic treatments

Photodynamic experiments were carried out using a modified version of a previously described method [14]. A431 or NHEK cells were seeded at a density of 1×10^6 cells/ml in T12.5 cm^2 flasks (with gas-tight caps, loosened; BD Falcon) and incubated at 37 °C under physioxia, using the method described above, or under hyperoxia, for 48 h prior to treatment. After the first 24 h, the culture medium was replaced, and the cells were placed back into the incubator under the same O_2 concentration. Following this incubation period, the culture medium was removed, and treatments were prepared in pre-gassed media, as described above. Cells were treated with MAL (1 mM) or ALA (0.5 mM) and the flasks were then incubated under physioxia or hyperoxia for 3 h at 37 °C. For the "physioxia + temporary hyperoxia" condition, cells were cultured and treated under physioxia and subsequently exposed to hyperoxia for the final 1 h of treatment and during irradiation (see Fig. 1A). Prior to irradiation, flask caps were tightened to maintain the internal atmosphere. Each flask was turned upside down and placed under the light source (Aktilite CL16; Galderma), set 10 cm above the flasks (see the schematic shown in Fig. S3) and irradiated for 5 min (hυ; 25 J/cm^2). Post-irradiation, flasks were washed, and fresh medium was added, followed by a further incubation under physioxia or hyperoxia for 3 h at 37 °C. Cells were then collected and washed in preparation for analysis of cell death and mitochondrial membrane potential. Where the effects of thioredoxin antioxidant system inhibitors on photodynamic cell killing were tested, cells were co-treated with 1 mM MAL in the absence or presence of non-toxic concentrations of each inhibitor, which consisted of: auranofin (Enzo Life Sciences), a thioredoxin reductase 1 and 2 chemical inhibitor [22];PX-12 (2-[(1-methylpropyl)dithio]-1H-imidazole; Tocris Bioscience), an irreversible selective thioredoxin-1 inhibitor [23]; thioredoxin-1 inhibitors PMX290 (4-(1-benzenesulfonyl-6-fluoro-1Hindol-2-yl)-4-hydroxy-cyclohexa-2,5-dienone; Abcam) [24,25] and PMX464 (4-(2-benzothiazolyl)-4-hydroxy-2,5-cyclohexadien-1-one; Tocris) [25,26] and conoidin A (Cayman Chemicals), a peroxiredoxin 1 and 2 inactivator [27]. Flow cytometry was carried out using Beckman Coulter Quanta SC and Merck Guava® easyCyte flow cytometers.

2.5. Cell death

Cell death was measured using a modified version of a previously published method [28]. In brief, washed cells were re-suspended in 100 µl of ice cold Ca^{2+} buffer containing 1.25 µg/ml annexin V-FITC (BioLegend). After 15 min on ice and in the dark, 900 µl of Ca^{2+} buffer containing 0.04 mg/ml propidium iodide (Sigma-Aldrich) was added to the cell suspension and the cells were ready to analyze by flow cytometry. Annexin V-FITC and propidium iodide stains were excited (488 nm) and emission was measured at 520 nm and 670 nm, respectively.

2.6. Mitochondrial membrane potential

Washed cells were re-suspended in 1 ml cold PBS containing 200 nM tetramethylrhodamine, methyl ester (TMRM; ThermoFisher) and incubated for 30 min at 37 °C in the dark, after which the cells were ready for analysis by flow cytometry. TMRM was excited (488 nm) and emission was measured at 575 nm.

2.7. Detection of photogenerated ROS by dihydroethidium and mito-dihydroethidium

Thirty minutes prior to irradiation, 10 µM dihydroethidium (DHE; Sigma-Aldrich) or 2.5 µM triphenylphosphonium-derivatized DHE

(mito-DHE; also known as MitoSOX; ThermoFisher) was added to each flask. Post-irradiation, cells were washed, collected and re-suspended in 1 ml of cold PBS ready for analysis by flow cytometry. Oxidation products of DHE and mito-DHE were excited (370 ± 30 nm) and emission was measured at 590 nm.

2.8. Detection of $^1O_2$ by electron paramagnetic resonance spectroscopy

All spectra were acquired using a Jeol JES-REX1 EPR spectrometer at room temperature [14]. Spectral acquisition settings were; microwave frequency 9.45 G, microwave power 4 mW, centre field 335.5 mT, sweep width 50 G, sweep time 100 s, time constant 1 s, modulation frequency 100 kHz and modulation width 1.25 G. The spectrum was acquired as a mean average of 3 spectral sweeps. The spin trap TMP (2,2,6,6-tetramethyl-4-piperidinol; Sigma-Aldrich) was used to trap $^1O_2$, forming TEMPOL (1-oxyl-2,2,6,6-tetramethyl-4- piperidinol) as the detectable spin adduct, which produces a three line spectrum with hyperfine splitting of aN = 16.3 G [30]. TMP was dissolved in 100% methanol to a concentration of 2 M. As a positive control for the trapping of $^1O_2$ by TMP, commercially available PpIX (10 μM; Sigma-Aldrich) and TMP (50 mM in PBS, pH 7.4) were injected into a Jeol LC-11 flat cell and irradiated (hυ; 25 J/cm^2) *in situ* in the EPR cavity. Spectra were acquired pre- and post-irradiation. Cells were trypsinized, washed twice, re-suspended in 0.5 ml DMSO, and incubated at room temperature for 10 min in the dark. The resulting lysate was centrifuged at 10,000g for 10 min and the supernatants were collected. Spectral acquisition and irradiation was carried out on the supernatants in the same manner as pure PpIX, described above.

2.9. Detection of lipid peroxidation by C11-BODIPY$^{581/591}$ and mito-C11-BODIPY$^{581/591}$

One hour prior to irradiation, 1 μM C11-BODIPY$^{581/591}$ (4,4-difluoro-5-(4-phenyl-1,3-butadienyl)-4-bora-3a,4a-diaza-s-indacene-3-undecanoic acid; ThermoFisher) or 100 nM mito-C11-BODIPY$^{581/591}$ (derived from C11-BODIPY$^{581/591}$, conjugated to a triphenylphosphonium lipophilic cation - also known as MitoPerOx, synthesized as previously described [29]) was added to each flask. The triphenylphosphonium conjugation leads to selective uptake of mito-C11-BODIPY$^{581/591}$ into mitochondria in cells [29]. Post-irradiation, cells were washed and re-suspended in 1 ml of cold PBS ready for analysis by flow cytometry. C11-BODIPY$^{581/591}$ and mito-C11-BODIPY$^{581/591}$ were excited (488 nm) and emissions were measured at 520 nm (oxidized form) and 575 nm (non-oxidized form).

2.10. Real time polymerase chain reaction for measuring gene expression

Cells were maintained under conditions of physioxia or hyperoxia for 48 h in 10 cm dishes, after which they were scraped into cold PBS and pelleted by centrifugation. RNA was extracted from cell pellets using the QIAamp RNA blood mini kit (Qiagen) as per the manufacturers' instructions. RNA concentration and purity was determined by measuring absorbance at 260 nm and 280 nm using a multi-sample NanoDrop 8000 (Thermo Scientific). Reverse transcription was carried out by mixing 100 ng of RNA with 8 μl 5X Variable Input Linear Output (VILO) and 4 μl 10X SuperScript® reverse transcriptase (Life Technologies), with the total volume made up to 40 μl with diethylpyrocarbonate-treated H_2O. Samples were then placed into a thermal cycler with the following temperature profile; 25 °C for 10 min, 42 °C for 60 min and 85 °C for 5 min. Each sample of cDNA was added to 100 μl TaqMan® Universal Master Mix II (Life Technologies) and 60 μl DEPC-H_2O. The master mix contained AmpliTaq® Gold DNA polymerase, optimized salts, deoxyribonucleotides (dNTP), buffers and a ROX™ dye as an internal reference. Each sample was gently mixed and loaded onto the array. Reactions were carried out on the TaqMan Low Density Array (TLDA) platform on the ABI Prism® 7900HT system (ThermoFisher). The amplification conditions were; 2 min at 50 °C, 10 min at 95 °C and 50 cycles of 30 s at 97 °C and 1 min at 59.7 °C (run time ~ 2.5 h). Data were handled in SDS Manager 2.3 and RQ Manager 1.2 and was subsequently analyzed using the Comparative Ct approach [31]. Expression data was normalized against the median expression of two control genes: *B2M* (beta-2-microglobulin) and *GUSB* (beta-glucuronidase). Repeated measurements were carried out for each condition and differences in gene expression were analyzed by two-tailed Student's *t*-test. As the genes were chosen on an *a priori* basis, no adjustments were made for the number of statistical tests carried out and therefore P values < 0.05 were considered statistically significant. Of the 28 genes targeted (Supplementary Table 1), all but 3 (*CPO*, *NOS2* and *NOX4*) were successfully amplified.

2.11. Cell lysis and protein isolation for enzyme activity assays

Lysates were prepared prior to carrying out antioxidant enzyme activity assays. A431 cells were cultured for 48 h under physioxia or hyperoxia in 10 cm dishes (Greiner), after which they were washed and scraped into 200 μl of ice cold 50 mM potassium phosphate (pH 7.4) containing 1 mM EDTA, collected in 1.5 ml Eppendorf tubes containing ceramic beads (Analytik Jena) and homogenized using a bead homogenizer (Analytik Jena). The crude mixture was transferred to new tubes and centrifuged at 10,000*g* for 15 min at 4 °C, after which the supernatant was transferred again and either stored on ice or frozen (− 80 °C) until used. Protein content was measured using the bicinchoninic acid (BCA) assay.

2.12. Superoxide dismutase activity

Superoxide dismutase (SOD) activity was measured, using the method described by Peskin and Winterbourn [32], by monitoring the hypoxanthine and xanthine oxidase-generated superoxide-dependent reduction of the tetrazolium dye, WST-1 ((2-(4-iodophenyl)-3-(4-nitrophenyl)-5-(2,4-disulfophenyl)-2H-tetrazolium sodium salt; Dojindo Molecular Technologies). In brief, assay buffer (50 mM sodium phosphate (pH 8.0) containing 0.1 mM DTPA (diethylenetriaminepentaacetic acid; Sigma-Aldrich), 0.1 mM hypoxanthine (Sigma-Aldrich) and 50 μM WST-1) was added to each well of a 96 well plate containing 100 μg of sample protein. The reaction was initiated by adding xanthine oxidase (Sigma-Aldrich, final activity 10 mU) and the plate was shaken vigorously for 30 s. WST-1 reduction was monitored by absorbance at 438 nm using a SpectraMax M2^e (Molecular Devices), at 25 °C. Known concentrations of bovine SOD (Sigma-Aldrich, 0–40 U/ml) were also assayed, allowing interpolation of the samples from a standard curve, where 1/slope of the initial linear reaction (ΔA_{438} 0–2 min) was plotted against SOD concentration.

2.13. Thioredoxin reductase activity

Thioredoxin reductase (TrxR) activity was measured, using a modified version of the method described by Tamura and Stadtman [33], by monitoring the NADPH-dependent reduction of DTNB (5,5′-dithiobis(2-nitrobenzoate)) to TNB (2-nitro-5-thiobenzoate). In brief, assay buffer (500 mM potassium phosphate (pH 7.0) containing 50 mM KCl, 10 mM EDTA and 0.2 mg/ml BSA) was added to each well of a 96 well plate containing 50 μg sample protein. Where applicable, DTNB was added to a final concentration of 10 mM and the reaction was initiated by adding NADPH to a final concentration 240 μM. The plate was shaken vigorously for 30 s and the reduction of DTNB was monitored by absorbance at 412 nm. One unit of TrxR is defined as the amount of enzyme that catalyzes the NADPH-dependent production of 2 μM of TNB per min at 22 °C, where the extinction coefficient of TNB at 412 nm is 13,600 M^{-1} cm^{-1}.

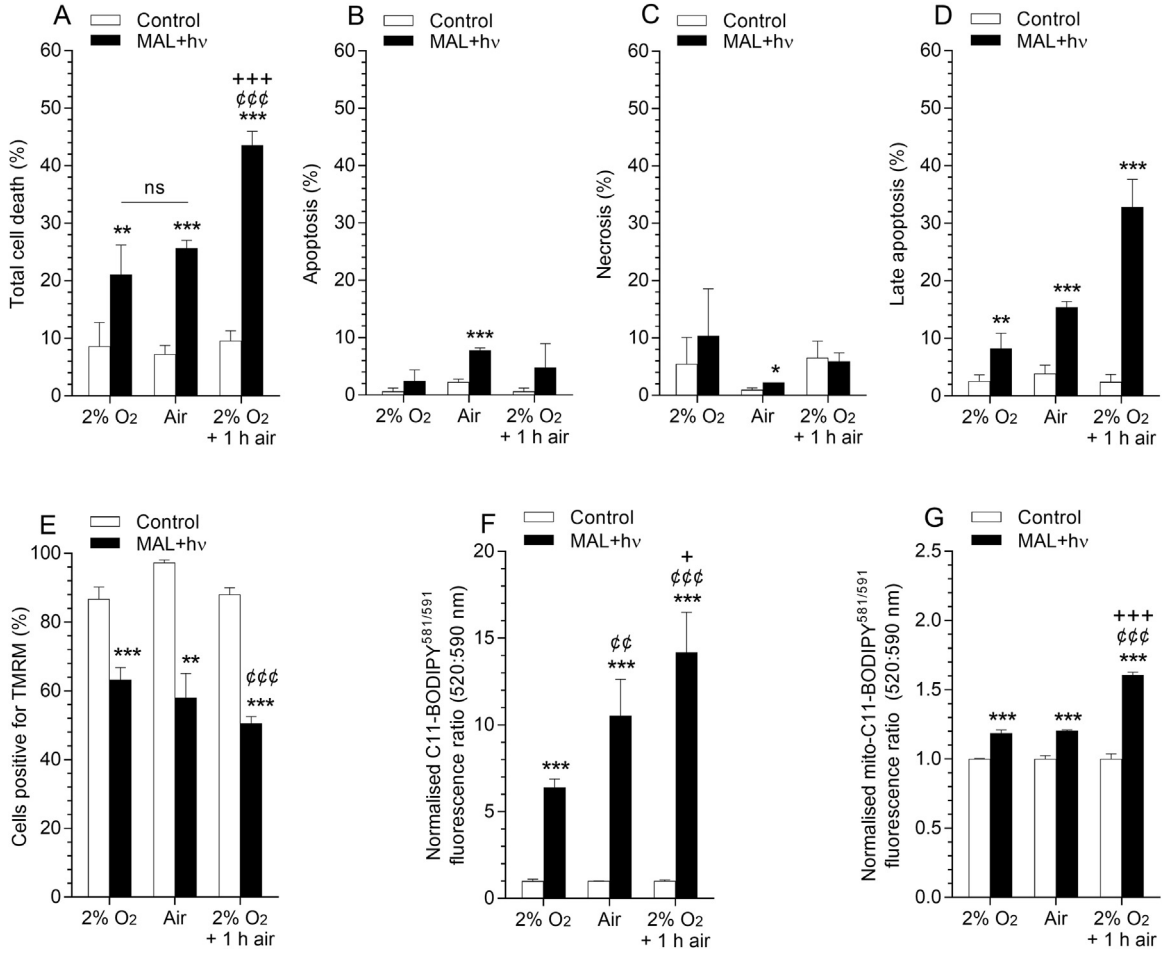

Fig. 2. The effects of physioxia and hyperoxia on photodynamic cell killing and subsequent changes to mitochondrial integrity and lipid peroxidation. Cell death, mitochondrial membrane potential and lipid peroxidation were assessed following treatment of A431 cells with 1 mM MAL and irradiation under conditions of "physioxia" (2% O_2), "hyperoxia" (air) or "physioxia + temporary hyperoxia" (2% O_2 + 1 h air), as indicated in Fig. 1A. A group of cells within each O_2 condition remained untreated ("control"), i.e. no pro-drug (MAL) addition nor photoirradiation. (A) Total cell death (annexin V-FITC and propidium iodide staining with flow cytometry; n = 5). (B) Apoptosis (cells stained with only annexin V-FITC). (C) Necrosis (cells stained with only propidium iodide). (D) Late apoptosis (cells dual-stained with both annexin V-FITC and propidium iodide). (E) Mitochondrial membrane potential (TMRM staining with flow cytometry; n = 4). (F-G) Whole-cell and mitochondrial lipid peroxidation detected by C11-BODIPY$^{581/591}$ or mito-C11-BODIPY$^{581/591}$ (also known as MitoPerOx) in conjunction with flow cytometry analysis, respectively (n = 4). * = $P < 0.05$, ** = $P < 0.01$, *** = $P < 0.001$, compared to controls. ¢¢ = $P < 0.01$, ¢¢¢ = $P < 0.001$, compared to the same treatment under "physioxia". + = $P < 0.05$, +++ = $P < 0.001$, compared to the same treatment under "hyperoxia". Data are presented as mean ± one standard deviation, with statistical significance determined by a two-tailed Student's *t*-test.

2.14. Glutathione reductase activity

GR activity was measured, using a modified version of the method described by Mannervik [34], by monitoring the NADPH-dependent reduction of oxidized glutathione (GSSG). In brief, assay buffer (200 mM potassium phosphate (pH 7.0) containing 2 mM EDTA, 1 mM GSSG and 200 μM NADPH) was added to each well of a 96 well plate containing 100 μg sample protein. The plate was shaken vigorously for 30 s and the oxidation of NADPH was monitored by absorbance at 340 nm. One unit of GR is defined as the amount of enzyme that catalyzes the reduction of 1 μM of GSSG per min, the equivalent to the oxidation of 1 μM of NADPH per min at 22 °C, where the extinction coefficient of NADPH at 340 nm is 6.2 $mM^{-1}cm^{-1}$.

2.15. Catalase activity

Catalase activity was measured, using the method described by Li and Schellhorn [35], by monitoring the decomposition of hydrogen peroxide (H_2O_2). Briefly, in a quartz cuvette 100 μg sample protein was added to 5 mM H_2O_2 in 50 mM phosphate buffer (pH 7.0) and absorbance was immediately monitored at 240 nm for 5 min at 22 °C. Catalase activity was calculated based on the rate of decrease of absorbance at 240 nm, which is proportional to the decomposition of H_2O_2.

2.16. Glutathione measurements

Reduced and oxidized glutathione were measured using a modified version of the Hissin and Hilf fluorometric method [36], where glutathione derivatisation was carried out using *o*-phthalaldehyde (*o*PA). Cell lysates were de-proteinised by incubating with 28% trichloroacetic acid on ice for 10 min. Following centrifugation at 14,000*g* for 15 min at 4 °C, supernatants were collected and assayed. For the measurement of reduced glutathione, 10 μl of the supernatant was mixed with 90 μl of buffer (100 mM sodium phosphate, 5 mM EDTA at pH 8.0). This mixture (20 μl) was then mixed with 425 μl of buffer and 25 μl of *o*PA (5 mg/ml) and then incubated at room temperature for 15 min. For the measurement of oxidized glutathione, 10 μl of the supernatant was mixed with 4 μl of N-ethylmaleimide (0.04 M) and incubated at room temperature for 30 min, after which 86 μl of NaOH (0.1 M) was added. This mixture (20 μl) was added to 45 μl of NaOH (0.1 M) and 10 μl of *o*PA (5 mg/ml) and incubated at room temperature for 15 min. Each

sample was pipetted into a 96 well plate, in duplicate, and fluorescence measurements were made using a SpectraMax M2^e plate reader. The concentrations of reduced and oxidized glutathione in each sample were determined by interpolation from standard curves of reduced and oxidized glutathione (Sigma-Aldrich; 0–10 μM) derivatized by *o*PA.

2.17. Resazurin microtitre assay

Clear-bottomed, black, 96-well plates were seeded with A431 cells at a density of 1.5×10^6 cells per ml (200 μl, 3×10^5 cells per well) and maintained under conditions of physioxia or hyperoxia for 48 h, prior to treatment with a concentration range of either 0–2 mM H_2O_2 or 0–50 μM auranofin prepared in DMEM. Following treatment, cells were washed with PBS, and then 5.5 μM resazurin (Sigma-Aldrich) prepared in fresh medium was applied. After 2 h of incubation at 37 °C, the fluorescence of the resorufin product was measured by fluorescence plate reader (excitation 571 nm, emission 585 nm).

2.18. Data analysis and statistics

Data are presented as mean ± one standard deviation of at least four replicates and *P* values were calculated using two-tailed Student's *t*-test for pairwise comparisons, unless otherwise stated.

3. Results

The majority of reported experiments were carried out with both MAL and ALA pro-drugs and the results were similar. Therefore, the results for experiments carried out with MAL are reported below (Figs. 1 and 2) and results for ALA can be found in the Supplementary Figs. (Figs. S4 and S5). Representative contour plots and histograms from flow cytometry data are presented in Fig. S6.

For clarity, where cells were exposed to different O_2 concentrations, we refer to different "O_2 conditions". A group of cells within each condition remained untreated ("control") to ensure that any observed effects were not due to the act of exposing cells to different O_2 conditions. Where cells were exposed to different pro-drugs and/or subjected to photo-irradiation, we have referred to different "treatments".

3.1. Measurement of O_2 within culture medium

The O_2 concentration of the media under the physioxic condition was measured (Fig. S2) at the beginning of culture (0 h), after a day of incubation (24 h) and prior to experimentation (48 h). At the beginning of culture, the O_2 concentration was 1.8 ± 0.7%. A small increase to 2.4 ± 0.7% (not statistically significant) was measured after 24 h of incubation. After a medium change and another 24 h incubation, the O_2 concentration was 2.1 ± 0.7%. The O_2 concentration of the media under air was 19.3 ± 1.0%.

3.2. Intracellular PpIX accumulation is significantly decreased by cell culture under physioxia compared to culture under hyperoxia

Initially, MAL-induced intracellular PpIX accumulation was measured under each O_2 condition in the absence of photoirradiation. PpIX accumulation was significantly different under each O_2 condition (hyperoxia > temporary hyperoxia > physioxia) for cells treated with MAL (Fig. 1B).

3.3. The photo-generation of reactive oxygen species reflects the accumulation of PpIX

Oxidation of dihydroethidium (DHE) and its mitochondria-targeted derivative, mito-DHE (MitoSOX Red), was used to measure the photo-generation of whole-cell (Fig. 1C) and mitochondria-localized (Fig. 1D) reactive oxygen species (ROS), respectively [37]. Under each of the three tested O_2 conditions, photodynamic treatment with MAL increased DHE oxidation, compared to the respective control for each O_2 condition (Fig. 1C). However, no significant differences in ethidium fluorescence were observed between treatments under each O_2 condition. Photodynamic treatment also significantly increased mito-DHE oxidation under each O_2 condition, compared with each O_2 condition's respective control (Fig. 1D). Furthermore, treatment-induced mito-DHE oxidation was significantly different between each O_2 condition (hyperoxia > temporary hyperoxia > physioxia).

Compared to the physioxic control group, the hyperoxic control group exhibited a small increase in mito-DHE oxidation (Fig. 1D), whilst there was no difference in the fluorescence of the control group under temporary hyperoxia compared to the physioxic control group. This confirms that "reperfusion events", characterized by increased "whole cell" (Fig. 1C) or mitochondrial (Fig. 1D) ROS production [38], did not occur in the physioxic condition.

Electron paramagnetic resonance (EPR) spectroscopy was used in conjunction with spin trapping to assess the photodynamic generation of $^1O_2$ by irradiated PpIX in cell lysates (Fig. 1E–I). 2,2,6,6-Tetramethylpiperidine (TMP) was used to trap generated $^1O_2$, forming the detectable spin adduct TEMPOL, which produces a three line spectrum with hyperfine splitting of aN = 16.3 G [30]. Photodynamic irradiation under each O_2 condition led to significant increases in TEMPOL formation (Fig. 1E-H) compared to the control group. The concentration of TEMPOL formed was determined by comparison to a standard curve (Fig. 1I). As with mito-DHE, TEMPOL formation was significantly different between each O_2 condition (Fig. 1E; hyperoxia > temporary hyperoxia > physioxia).

3.4. Cells cultured long-term under hyperoxic conditions are resistant to photodynamic cell killing

In phenotypically identical cells, elevated PpIX accumulation and ROS levels in hyperoxic cells, compared with physioxic cells, would be expected to translate to increased damage to, and killing of, the hyperoxic cells [39]. To test this, cell death, mitochondrial integrity and lipid peroxidation were assessed (Fig. 2). No significant difference was observed in the extent of cell death of controls (Fig. 2A) or dark toxicity controls (treatment with MAL in the absence of irradiation; Fig. S7) under each O_2 condition. Following photodynamic treatments, cell death significantly increased under each O_2 condition (Fig. 2A). No significant differences in cell death were observed between photodynamic treatments under physioxia and hyperoxia. Photodynamic treatment under temporary hyperoxia resulted in significant increases in cell death compared to equivalent treatments under physioxia and hyperoxia (Fig. 2A). No statistically significant correlation was found between PpIX accumulation and photodynamic cell killing. Annexin V-FITC and propidium iodide staining allowed the identification of apoptotic and necrotic populations of cells (Fig. 2B–D). Cells identified as "late apoptotic" (dual stained; Fig. 2D) accounted for the largest proportion of dead cells and exhibited the largest changes following treatment, whilst cells stained with either annexin V-FITC ("apoptotic"; Fig. 2B) or propidium iodide ("necrotic"; Fig. 2C) alone exhibited smaller changes following treatment. Normal human epidermal keratinocytes (NHEK) did not exhibit any significant changes in cell death under each O_2 condition following photodynamic treatment (Fig. S8). The lack of NHEK susceptibility to PpIX-based photodynamic cell killing under different conditions has previously been reported [40,41].

Mitochondrial membrane potential (ΔΨm) was assessed by TMRM staining, to determine treatment-induced mitochondrial damage. Significant decreases in ΔΨm were observed following photodynamic treatments (Fig. 2E) and ΔΨm positively correlated with total cell death (r^2 = 0.89, P = 0.0001). Lipid peroxidation following photodynamic treatments was assessed using the probe C11-BODIPY$^{581/591}$ (Fig. 2F) and its mitochondria-targeted derivative mito-C11-BODIPY$^{581/591}$ (MitoPerOx [29], Fig. 2G). Oxidation of C11-BODIPY$^{581/591}$ and mito-C11-

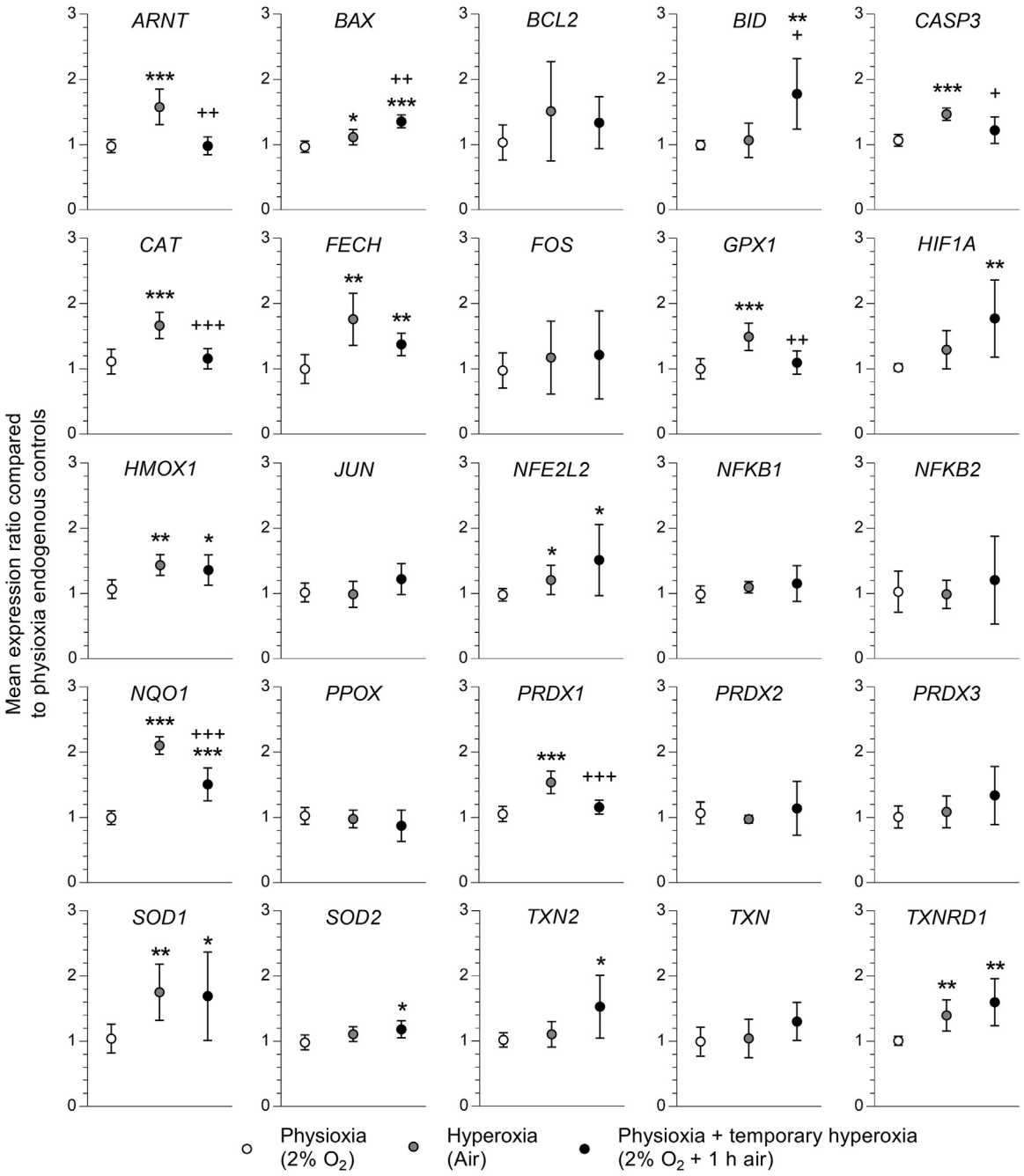

Fig. 3. The effects of culturing A431 cells under physioxia or hyperoxia on gene expression. Expression of genes in A431 cells cultured under physioxia (2% O_2), hyperoxia (air) or physioxia + temporary hyperoxia (2% O_2 + 1 h air) as indicated in Fig. 1A. Gene abbreviations: Aryl hydrocarbon receptor nuclear translocator (*ARNT*); Bcl-2-associated X protein (*BAX*); B-cell lymphoma 2 (*BCL2*); BH3 interacting-domain death agonist (*BID*); caspase 3 (*CASP3*); catalase (*CAT*); ferrochelatase (*FECH*); c-Fos (*FOS*); glutathione peroxidase 1 (*GPX1*); hypoxia-inducible factor 1α (*HIF1A*); heme oxygenase (*HMOX*); c-Jun (*JUN*); Nrf-2 (nuclear factor (erythroid-derived 2)-like 2 (*NFE2L2*)); nuclear factor NF-kappa-B p105 subunit (*NFKB1*) and p100 subunit (*NFKB2*); NADPH quinone oxidoreductase (*NQO1*); protoporphyrinogen oxidase (*PPOX*); peroxiredoxin 1–3 (*PRDX1–3*); superoxide dismutases 1 and 2 (*SOD1, SOD2*); thioredoxins 1 and 2 (*TXN, TXN2*) and thioredoxin reductase 1 (*TXNRD1*). * = $P < 0.05$, ** = $P < 0.01$, *** = $P < 0.001$, compared to physioxia. + = $P < 0.05$, + + = $P < 0.01$, + + + = $P < 0.001$, compared to hyperoxia. Data are presented as mean ± 95% confidence intervals, with statistical significance determined by a two-tailed Student's *t*-test; n = 6–8.

$BODIPY^{581/591}$ increased under each O_2 condition and correlated positively with cell death ($r^2 = 0.95$, P = 0.0008; $r^2 = 0.97$, $P = 0.0003$, respectively).

3.5. Adaptation to hyperoxic conditions significantly enhances basal cellular redox defences, conferring resistance to oxidative stressors

Similar levels of cellular damage and death were observed following photodynamic treatment under the physioxic and hyperoxic conditions (Fig. 2), despite significant differences in PpIX accumulation and ROS generation (Fig. 1). The data presented thus far provide evidence that cells cultured under hyperoxia and physioxia might have quantitative differences in the levels of their antioxidant defences required for protection against treatment-induced oxidative stress. A Taqman® low-density array platform was used to assess the expression of selected genes following the culture of cells under each O_2 condition (Fig. 3). Genes were selected for analysis *a priori,* based on their potential roles in PpIX-based photodynamic cell killing, such as antioxidant defence

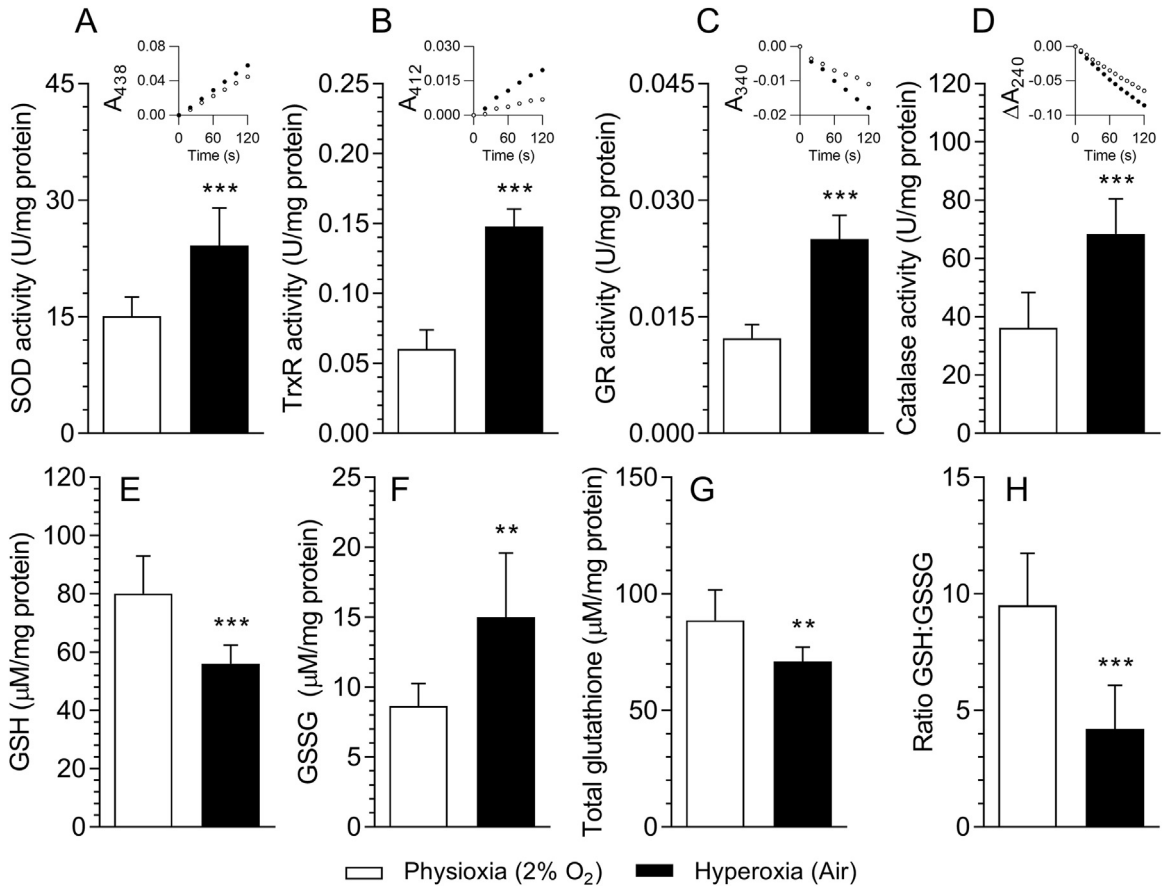

Fig. 4. The effects of culturing A431 cells under physioxia or hyperoxia on antioxidant enzyme activities and glutathione levels. Cells were cultured under physioxia (2% O_2) or hyperoxia (air) for 48 h, as indicated in Fig. 1A, and lysates were subsequently measured for antioxidant enzyme activities. (A) Superoxide dismutase (SOD) activity. (B) Thioredoxin reductase (TrxR) activity. (C) Glutathione reductase (GR) activity. (D) Catalase activity. Each inset graph is representative of the absorbance time-course for each assay (n = 8). (E) Reduced glutathione (GSH). (F) Oxidized glutathione (GSSG). (G) Total glutathione (GSH + GSSG). (H) GSH:GSSG ratio (n = 12). Data are presented as mean ± one standard deviation. ** = $P < 0.01$, *** = $P < 0.001$ determined by two-tailed Student's *t*-test.

(*e.g. CAT, GPX1, PRDX1* and *TXN* [42–45]), apoptosis (*e.g. CASP3, BCL2* and *BAX* [46]) and haem biosynthesis (*e.g. PPOX, CPO* and *FECH* [47]). Additionally, genes that may be affected or regulated by O_2 concentration were selected (*e.g. HMOX1, NFE2L2* and *TXNRD1* [48,49]). Of the 28 genes assessed (Supplementary Table 1) 17 were found to have statistically significant differences in expression (Fig. 3; $P < 0.05$, two-tailed Student's *t*-test) between each O_2 environment. The expression of *BAX*, *CASP3*, *FECH*, *ARNT, NFE2L2* (Nrf-2), *HMOX1*, *CAT*, *GPX1*, *NQO1*, *SOD1*, *PRDX1* and *TXNRD1* was higher under hyperoxia compared to physioxia. These data suggest that cells cultured under hyperoxia are adapted to cope with oxidative stress (in this instance, induced by the PpIX-dependent photodynamic treatment) through greater expression of key antioxidant genes. Under temporary hyperoxia, the expression of *BAX*, *BID*, *NFE2L2*, *HMOX1*, *NQO1*, *SOD1*, *SOD2*, *TXN2* and *TXNRD1* was significantly increased compared to physioxia, suggesting a response by physioxic cells to hyperoxia-induced oxidative stress. Differences in antioxidant gene expression were reflected by differences in antioxidant enzyme activity (Fig. 4A-D). Under hyperoxia, the activities of superoxide dismutase, thioredoxin reductase, glutathione reductase and catalase were significantly higher compared to physioxia. Additionally, under hyperoxia, cells had significantly less reduced glutathione (GSH; Fig. 4E) and more oxidized glutathione (GSSG; Fig. 4F) compared to physioxia. Cells under hyperoxia also had significantly less total glutathione (Fig. 4G). The ratio of GSH:GSSG (Fig. 4H) was significantly higher under physioxia compared to hyperoxia.

Cells were also exposed to alternative oxidative stressors to establish whether these observations could be considered broadly, or if they were specific to photodynamic-induced oxidative stress. Following culture under the physioxic or hyperoxic O_2 conditions, cells were treated with either hydrogen peroxide (H_2O_2; Fig. 5A) or the thioredoxin reductase inhibitor auranofin (Fig. 5B) for a further 24 h to induce toxicity. Compared to cells treated under hyperoxia, physioxic cells were less viable when treated with 1–2 mM H_2O_2 and 12.5–50 μM auranofin. Lipid oxidation, as measured by C11-BODIPY$^{581/591}$ (Fig. 5C), was greater under physioxia compared to hyperoxia over 24 h. When treated with cumene hydroperoxide (an inducer of lipid oxidation) for 30 min, lipid oxidation increased 8.2-fold under physioxia, but only 1.8-fold under hyperoxia. Mitochondrial ROS generation, as measured by mito-DHE (Fig. S9) was also significantly higher under physioxia compared to hyperoxia, over 24 h.

3.6. Inhibitors and inactivators of the thioredoxin antioxidant system increase photodynamic treatment efficacy under physioxia, but not hyperoxia

The above gene expression data, as well as the enzyme activity measurements, suggested that a set of antioxidant genes was upregulated by the long-term culture of cells under air, compared with 2% O_2. To further probe, at the protein level, the potential molecular pathways involved in the hyperoxia-induced resistance of cells to photodynamic irradiation, we performed pharmacological experiments by testing the effects of thioredoxin antioxidant system inhibitors on photodynamic cell killing. Cells were co-treated with 1 mM MAL and each inhibitor/inactivator at a concentration found to be non-toxic on their own (Fig. 6A). These compounds included the thioredoxin reductase

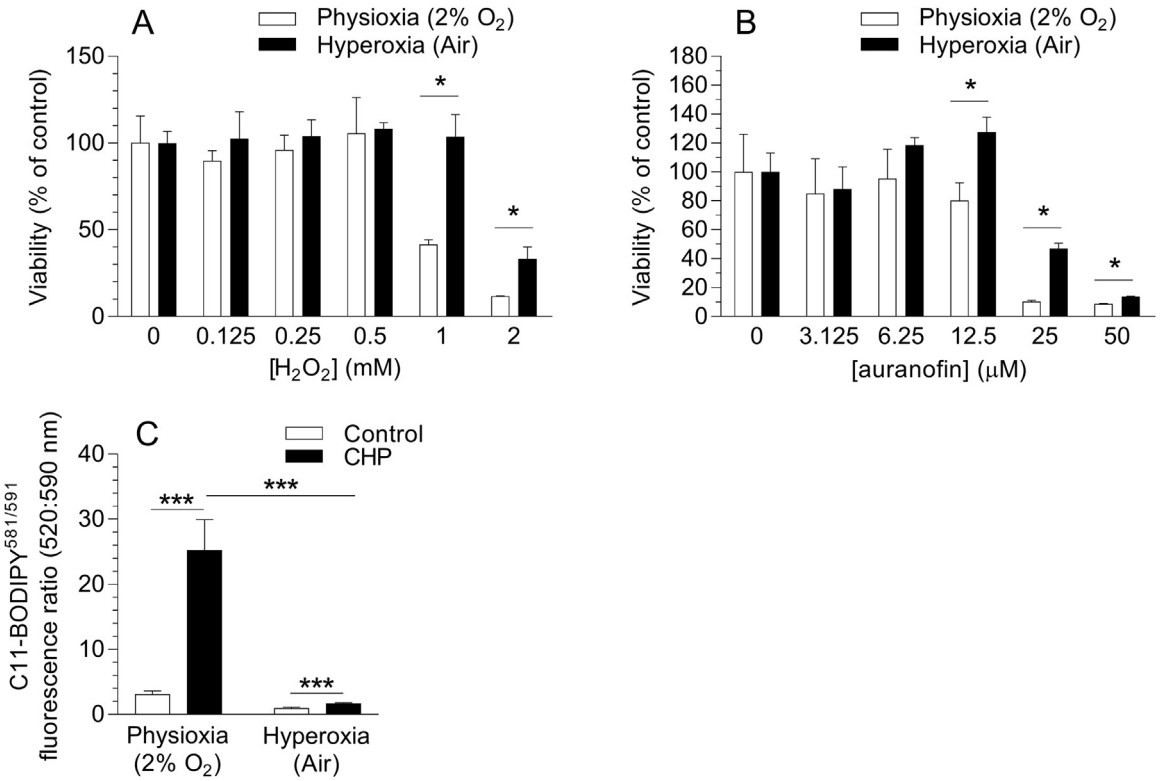

Fig. 5. The effects of culturing A431 cells under physioxia or hyperoxia on the cellular response to treatment with oxidative stressors. Cells were cultured under physioxia (2% O_2) or hyperoxia (air) for 48 h, as indicated in Fig. 1A, and subsequently subjected to treatment with oxidative stressors. (A and B) Cell viability (resazurin metabolic activity assay) was measured after 24 h treatment with H_2O_2 (0–2 mM) or auranofin (0–50 μM; n = 5). (C) Cells were incubated with C11-BODIPY$^{581/591}$ for 24 h. After 24 h, one group of cells was treated with cumene hydroperoxide (CHP; 50μM) for 30 min prior to measurement of the C11-BODIPY$^{581/591}$ product fluorescence by flow cytometry. In a second group of "control" cells (not treated with CHP), baseline whole cell lipid oxidation was determined, again by the measurement of C11-BODIPY$^{581/591}$ product fluorescence by flow cytometry. Data are presented as mean ± one standard deviation. * = $P < 0.05$, *** = $P < 0.001$, determined by a two-tailed Student's *t*-test.

inhibitor auranofin (1 μM), the thioredoxin-1 inhibitors PX12 (10 μM), PMX290 (1 μM), PMX464 (1 μM) and the peroxiredoxin-1/2 inactivator conoidin A (10 μM). Following co-treatment for 3 h, cells were subjected to photodynamic irradiation as before. Each inhibitor significantly potentiated MAL-based photodynamic cell killing under physioxia, whilst having no significant effect under hyperoxia (Fig. 6B). Further experiments showed that the potentiation under physioxia was not driven by increases in PpIX accumulation (Fig. 6C) and that auranofin and PX12 appeared to increase photo-generated mitochondrial ROS (Fig. 6D).

4. Discussion

We have demonstrated that the basal redox defence mechanisms of skin cells cultured *in vitro* were significantly influenced by the O_2 condition under which they were cultured and that adaptation to the condition over 48 h influenced subsequent cellular responses to treatment-induced oxidative stress. Our experiments revealed that the culture of cells in a physiologically relevant O_2 condition (2% O_2) decreased the expression of Nrf2-regulated antioxidant defence genes and other antioxidant genes, in turn leading to decreased antioxidant enzyme activities. Moreover, it appears that the culture of cells under air (18.6% O_2) imparts an "artefactual" resistance to treatment-induced oxidative stress. This investigation provides new insights into the effects of physioxic cell culture on photodynamic cell killing, and associated pathways, in a model of a clinically relevant treatment.

Previous *in vitro* investigations [6,50,51] have focused on the effects of low O_2 typical of diseases *in vivo* [52–54]. However, cells treated under these conditions were often compared to cells cultured under air, incorrectly inferring that this oxygenation was representative of "healthy" tissues, and studies have often used short-term decreases in O_2 concentration [4,5], rather than longer periods associated with disease. Additionally, air has been used to represent post-reperfusion oxygenation when modelling reperfusion events *in vitro* [55,56].

It has been reported that culturing of a variety of healthy cell types under physioxia produced phenotypes closer to those observed *in vivo* [57–60] compared to cells cultured under air. Culture under physioxia enhanced clonal growth [61–63] and the generation of cytokines by blood mononuclear cells [59,63]. Culturing stem cells under physioxia improved proliferation [58,60], whilst culturing stem-like cells under physioxia improved the development of stem cell characteristics [57], compared to culture under air.

In the present study, the resistance of cells cultured under air to oxidative stress-induced cell death was revealed by an absence of an anticipated correlation between cell death and either PpIX accumulation or ROS generation. Photodynamic cell killing is dependent on three factors: O_2 concentration, photosensitiser concentration and photoirradiation energy [64]. Therefore, given that the irradiation conditions were identical for each treatment, it was surprising to observe no difference in cell death between the physioxic and hyperoxic conditions (Fig. 2A), despite the significant differences in O_2 concentration, PpIX concentration and ROS generation (Fig. 1B-I). In contrast to previous *in vitro* photodynamic experiments where low O_2 was demonstrated to decrease treatment efficacy [16,65,66], the current study revealed that cells cultured chronically in a physioxic environment were more susceptible to treatment-induced oxidative stress. It is likely that the previous studies [16,65,66] required cells to be cultured under - and presumably adapted to - hyperoxic conditions (air) prior to acute periods of low O_2 during short treatment phases.

In vivo studies have demonstrated an improved efficacy of

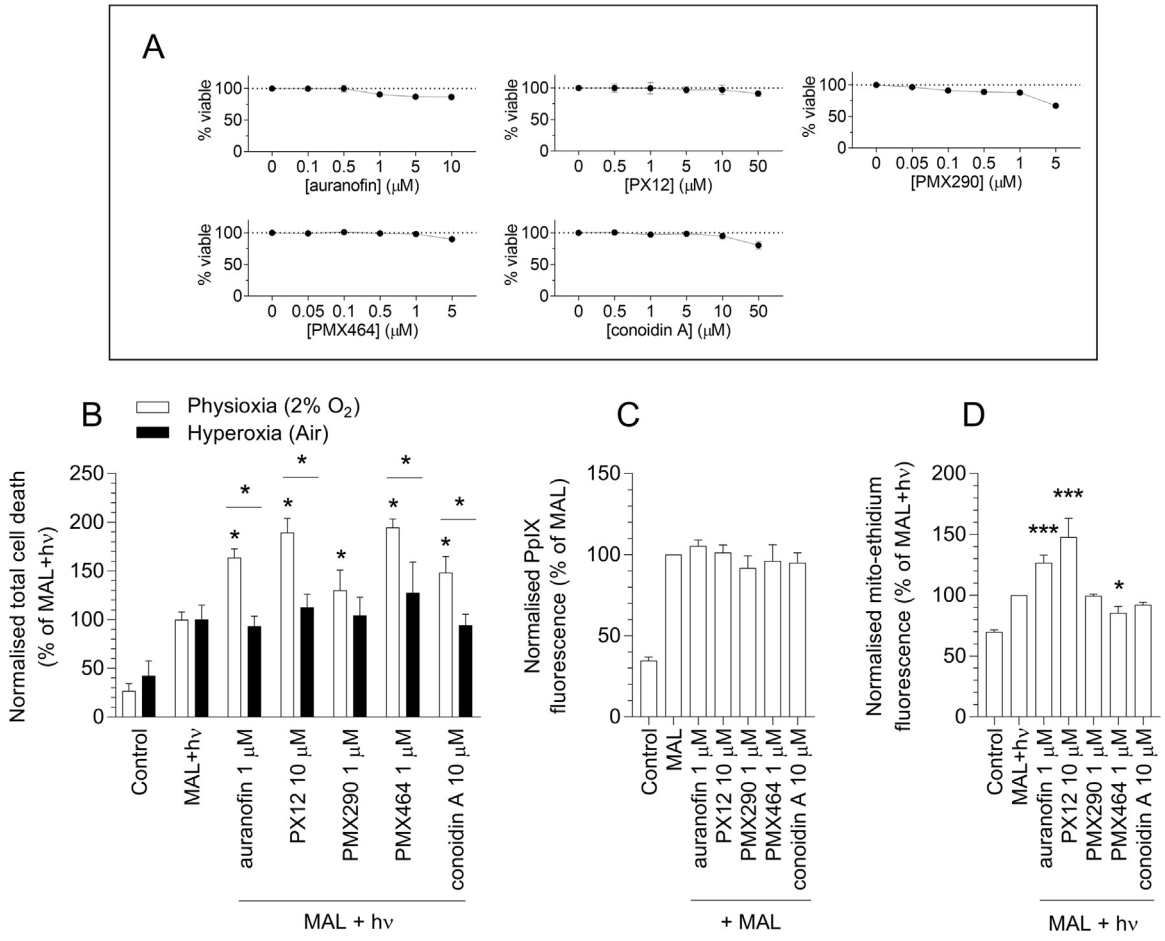

Fig. 6. The effects of inhibitors of the thioredoxin antioxidant system on photodynamic cell killing of A431 cells under physioxia or hyperoxia. Cells were cultured under physioxia (2% O_2) or hyperoxia (air) for 48 h, as indicated in Fig. 1A, and subsequently subjected to treatments. (A) Dark toxicity of inhibitors under physioxia for 24 h (n = 3–5). (B) Total cell death (annexin V-FITC and propidium iodide staining with flow cytometry) following treatment of cells with 1 mM MAL ± inhibitors (3 h) and irradiation (n = 4). (C) PpIX accumulation under physioxia was measured following treatment (3 h) with 1 mM MAL ± inhibitors (n = 4). (D) Photo-generated ROS under physioxia were detected by mito-DHE staining (n = 4). In (B-D), a group of cells within each O_2 condition remained untreated ("control"), i.e. no pro-drug (MAL) addition nor photo-irradiation. * indicates significance compared to the control group or where indicated by horizontal bars. Data are presented as mean ± one standard deviation. * = $P < 0.05$, *** = $P < 0.001$, determined by two-tailed Student's *t*-test.

photodynamic therapies by temporarily increasing O_2 availability [8,19], but *in vitro* studies have failed to replicate this [7]. Here, we have recapitulated the treatment-enhancing effects of temporary hyperoxia observed *in vivo* [8,19] by exposing cells to a short period of hyperoxia during treatment, following chronic culture under physioxia (Figs. 1 and 2). Interestingly, exposing physioxic cells to temporary hyperoxia resulted in significantly more photodynamic cell killing compared to chronically hyperoxic cells, despite identical concentrations of O_2 during irradiation and less PpIX and ROS in the temporary hyperoxia condition. This provided evidence of a fundamental difference between cells cultured under physioxia and hyperoxia, whereby cells under hyperoxia exhibit a phenotype associated with resistance to oxidative stress. A similar phenomenon has been reported in murine leukaemia (LBR) cell lines exposed to PpIX-based photodynamic killing [67]. Compared to doxorubicin and vincristine resistant lines, parent LBR cells exhibited the lowest level of mitochondrial dysfunction post-treatment, despite generating the highest level of ROS. In contrast, the efficacy of PpIX-dependent photodynamic treatments has been shown to correlate with photo-generated ROS, oxidative damage and cell death when the cells concerned are phenotypically similar [68,69].

Under hyperoxia, cells expressed significantly higher levels of genes coding for proteins linked to maintaining cellular redox homeostasis, including several key antioxidants and the oxidative stress-activated transcription factor Nrf2 (Fig. 3), with increased expression of NQO1 and HMOX1 mRNA indicating elevated Nrf2 activity [70]. Importantly, the activities of key antioxidant enzymes involved in maintaining redox homeostasis and protecting against oxidative stress were significantly higher in cells cultured under hyperoxia (Fig. 4) and have previously been shown to confer resistance to photodynamic therapy, chemotherapy and radiotherapy both *in vitro* and *in vivo* [42–45,71–73]. Further investigation found that selective inhibitors of the Nrf2-regulated thioredoxin antioxidant system increased the efficacy of photodynamic cell killing under physioxia, but not under hyperoxia (Fig. 6B) in a manner that was independent of PpIX accumulation (Fig. 6C). This is an important observation as, if these experiments had been carried out only in cells which had been cultured, long term, under hyperoxia (without inclusion of the long-term culture of cells at other O_2 concentrations), we would have concluded that the thioredoxin antioxidant system was not a valid target for increasing photodynamic cell killing. By targeting enzymes that comprise the thioredoxin antioxidant system, we have been able to demonstrate that this important pathway [74] is, in part, responsible for the resistance to oxidative stress-induced damage and cell death observed in cells cultured under hyperoxia. Cells cultured under hyperoxia also had a lower ratio of GSH:GSSG (Fig. 4H), providing further evidence that cells cultured under the hyperoxic conditions of atmospheric air exist in a persistent state of oxidative stress. Together, our findings provide an explanation as to why cells cultured under physioxia and hyperoxia respond to PpIX-based

photodynamic cell killing in a manner that does not agree with previous investigations [7,16,65,66,68,69]. Additional data (Fig. 5) demonstrated that our findings were not limited to photodynamic cell killing, with cells cultured long-term under the hyperoxic condition demonstrating resistance to cumene hydroperoxide-induced lipid peroxidation and drug-induced cell death.

Chapple et al. [75] have reported that Nrf2 activity was attenuated in human primary endothelial cells adapted to physioxia (5% O_2) compared to cells cultured under air. Significant changes in Nrf2-regulated redox signalling were observed after one day of physioxic culture and these changes were maintained through long-term (five-day) culture. Chapple et al. [75] also reported evidence of an O_2 gradient within *in vitro* cultures which could lead to the unintentional induction of hypoxia. The lack of effect on HIF1α expression (Fig. 3) of our physioxic condition indicates that hypoxia was not induced, but the possible existence of an O_2 gradient within our cultures should be considered in future work. Haas et al. [76] reported that the long-term culture of macrophages under 5% O_2 attenuated the immunomodulatory response to dimethyl fumarate and cells cultured under air exhibited a "pro-oxidant" phenotype (*i.e.* lower GSH:GSSG ratio), which is in agreement with our present observations. Our data support the theory that cells cultured under hyperoxic conditions (air) are in a persistent state of oxidative stress. We propose that the phenotype described here (elevated antioxidant gene expression and enzyme activity) is a necessary adaptation for these cells to survive in a high O_2 environment, which in turn affects how cells respond to experimental treatments. The heterogeneity in tissue oxygenation of both healthy and diseased tissues is well documented [77] and therefore the use of a single oxygen concentration to represent physioxia is potentially a limiting factor in the present study. Future *in vitro* investigations may benefit from studying a range of physiologically-relevant oxygen concentrations to understand the full scope of cellular responses within a tissue of interest.

In conclusion, we found that the standard *in vitro* O_2 conditions (air) placed cultured cells in a constant state of oxidative stress, arising from their culture under a hyperoxic environment. As such, the majority of *in vitro* cell culture experiments in contemporary laboratories are undertaken in oxidatively stressed cells. Culture in these conditions confers a protective resistance to PpIX-based photodynamic cell killing (and other oxidative stressors), which in turn could be considered an artefact of current standard cell culture conditions that contributes to a poor translation of *in vitro* investigations into *in vivo* investigations. Finally, the present experiments – by "pre-conditioning" cells under physioxia – rendered the levels of antioxidant enzyme activities and redox homeostasis more akin to those observed *in vivo* [20,78]. We observed that, by exposing cells cultured under physioxia to temporary hyperoxia, a higher concentration of ROS was generated in a cellular environment with a lower basal redox defence, thus causing more damage to cellular components and ultimately leading to an increased treatment effect. These observations should be considered particularly in relation to experiments investigating the effects of changes in O_2 concentration on functional parameters in cultured cells. The chronic culture of mammalian cells under a physiologically relevant O_2 concentration, prior to the exposure of such cells to stimuli or drugs should be incorporated into standard protocols for cell culture experiments, and we have demonstrated here that this is relatively easy and inexpensive to achieve.

Acknowledgements

This work was financially supported by DDRC Healthcare, UK, the Peninsula College of Medicine and Dentistry, UK. We would also like to thank the University of Exeter for HEIF Proof of Concept Funding. P.G.W., A.C. and D.C.J.F. are named inventors on pending patent applications stemming from an initial patent filing made in 2014, and relating to compounds for adjunctive PDT including thioredoxin reductase inhibitors such as auranofin.

Appendix A. Supplementary material

Supplementary data associated with this article can be found in the online version at doi:10.1016/j.freeradbiomed.2018.08.025.

References

[1] T.L. Place, F.E. Domann, A.J. Case, Limitations of oxygen delivery to cells in culture: an underappreciated problem in basic and translational research, Free Radic. Biol. Med. 113 (2017) 311–322.
[2] R.H. Wenger, et al., Frequently asked questions in hypoxia research, Hypoxia 3 (2015) 35–43.
[3] P.J. Sheffield, Measuring tissue oxygen tension: a review, Undersea Hyperb. Med. 25 (3) (1998) 179–188.
[4] H. Onozuka, K. Tsuchihara, H. Esumi, Hypoglycemic/hypoxic condition in vitro mimicking the tumor microenvironment markedly reduced the efficacy of anticancer drugs, Cancer Sci. 102 (5) (2011) 975–982.
[5] I. Georgakoudi, P.C. Keng, T.H. Foster, Hypoxia significantly reduces aminolaevulinic acid-induced protoporphyrin IX synthesis in EMT6 cells, Br. J. Cancer 79 (9–10) (1999) 1372–1377.
[6] D.L. Berge, et al., Chronic hypoxia modulates tumour cell radioresponse through cytokine-inducible nitric oxide synthase, Br. J. Cancer 84 (8) (2001) 1122–1125.
[7] A. Hjelde, et al., Lack of effect of hyperoxia on photodynamic therapy and lipid peroxidation in three different cancer cell lines, Med. Sci. Monit. 11 (10) (2005) Br351–Br356.
[8] M. Jirsa Jr.et al., Hyperbaric oxygen and photodynamic therapy in tumour-bearing nude mice, Eur. J. Cancer 27 (1) (1991) 109.
[9] S. Koch, et al., Efficacy of cytotoxic agents used in the treatment of testicular germ cell tumours under normoxic and hypoxic conditions in vitro, Br. J. Cancer 89 (11) (2003) 2133–2139.
[10] M. Jiang, et al., Autophagy is a renoprotective mechanism during in vitro hypoxia and in vivo ischemia-reperfusion injury, Am. J. Pathol. 176 (3) (2010) 1181–1192.
[11] H.L. Zhu, et al., Ischemic postconditioning protects cardiomyocytes against ischemia/reperfusion injury by inducing MIP2, Exp. Mol. Med. 43 (8) (2011) 437–445.
[12] S. Guo, et al., A cell-based phenotypic assay to identify cardioprotective agents, Circ. Res. 110 (7) (2012) 948–957.
[13] P. Agostinis, et al., Photodynamic therapy of cancer: an update, CA- Cancer J. Clin. 61 (4) (2011) 250–281.
[14] D.C.J. Ferguson, et al., The hydroxypyridinone iron chelator CP94 increases methyl-aminolaevulinate-based photodynamic cell killing by increasing the generation of mitochondrial reactive oxygen species, Redox Biol. 9 (2016) 90–99.
[15] A. Lomas, J. Leonardi-Bee, F. Bath-Hextall, A systematic review of worldwide incidence of nonmelanoma skin cancer, Br. J. Dermatol. 166 (5) (2012) 1069–1080.
[16] L. Wyld, M.W.R. Reed, N.J. Brown, The influence of hypoxia and pH on aminolaevulinic acid-induced photodynamic therapy in bladder cancer cells in vitro, Br. J. Cancer 77 (10) (1998) 1621–1627.
[17] S.M. Evans, et al., Oxygen levels in normal and previously irradiated human skin as assessed by EF5 binding, J. Invest. Dermatol. 126 (12) (2006) 2596–2606.
[18] E. Blake, et al., Effect of an oxygen pressure injection (OPI) device on the oxygen saturation of patients during dermatological methyl aminolevulinate photodynamic therapy, Lasers Med. Sci. 28 (3) (2013) 997–1005.
[19] Q. Chen, et al., Improvement of tumor response by manipulation of tumor oxygenation during photodynamic therapy, Photochem. Photobiol. 76 (2) (2002) 197–203.
[20] Y. Shindo, et al., Enzymic and non-enzymic antioxidants in epidermis and dermis of human skin, J. Investig. Dermatol. 102 (1) (1994) 122–124.
[21] M. Wang, et al., Manganese superoxide dismutase suppresses hypoxic induction of hypoxia-inducible factor-1alpha and vascular endothelial growth factor, Oncogene 24 (55) (2005) 8154–8166.
[22] A.G. Cox, et al., The thioredoxin reductase inhibitor auranofin triggers apoptosis through a Bax/Bak-dependent process that involves peroxiredoxin 3 oxidation, Biochem. Pharmacol. 76 (9) (2008) 1097–1109.
[23] A.F. Baker, et al., The antitumor thioredoxin-1 inhibitor PX-12 (1-methylpropyl 2-imidazolyl disulfide) decreases thioredoxin-1 and VEGF levels in cancer patient plasma, J. Lab Clin. Med. 147 (2) (2006) 83–90.
[24] J.M. Berry, et al., Quinols as novel therapeutic agents. 2.(1) 4-(1-Arylsulfonylindol-2-yl)-4-hydroxycyclohexa-2,5-dien-1-ones and related agents as potent and selective antitumor agents, J. Med. Chem. 48 (2) (2005) 639–644.
[25] D.T. Jones, et al., Novel thioredoxin inhibitors paradoxically increase hypoxia-inducible factor-alpha expression but decrease functional transcriptional activity, DNA binding, and degradation, Clin. Cancer Res. 12 (18) (2006) 5384–5394.
[26] G. Wells, et al., 4-Substituted 4-hydroxycyclohexa-2,5-dien-1-ones with selective activities against colon and renal cancer cell lines, J. Med. Chem. 46 (4) (2003) 532–541.
[27] J.D. Haraldsen, et al., Identification of conoidin A as a covalent inhibitor of peroxiredoxin II, Org. Biomol. Chem. 7 (15) (2009) 3040–3048.
[28] J.M. Tarr, et al., Extracellular calreticulin is present in the joints of patients with rheumatoid arthritis and inhibits FasL (CD95L)-mediated apoptosis of T cells, Arthritis Rheum. 62 (10) (2010) 2919–2929.
[29] T.A. Prime, et al., A ratiometric fluorescent probe for assessing mitochondrial phospholipid peroxidation within living cells, Free Radic. Biol. Med. 53 (3) (2012) 544–553.
[30] L.Y. Zang, Z.Y. Zhang, H.P. Misra, EPR studies of trapped singlet oxygen (1O2)

generated during photoirradiation of hypocrellin A, Photochem. Photobiol. 52 (4) (1990) 677–683.
[31] M.W. Pfaffl, A new mathematical model for relative quantification in real-time RT-PCR, Nucleic Acids Res. 29 (9) (2001) e45.
[32] A.V. Peskin, C.C. Winterbourn, A microtiter plate assay for superoxide dismutase using a water-soluble tetrazolium salt (WST-1), Clin. Chim. Acta 293 (1–2) (2000) 157–166.
[33] T. Tamura, T.C. Stadtman, A new selenoprotein from human lung adenocarcinoma cells: purification, properties, and thioredoxin reductase activity, Proc. Natl. Acad. Sci. USA 93 (3) (1996) 1006–1011.
[34] B. Mannervik, Measurement of glutathione reductase activity, Curr. Protoc. Toxicol. (2001) (**Chapter 7**: p. Unit7 2).
[35] Y. Li, H.E. Schellhorn, Rapid kinetic microassay for catalase activity, J. Biomol. Tech. 18 (4) (2007) 185–187.
[36] P.J. Hissin, R. Hilf, A fluorometric method for determination of oxidized and reduced glutathione in tissues, Anal. Biochem. 74 (1) (1976) 214–226.
[37] K.M. Robinson, et al., Selective fluorescent imaging of superoxide in vivo using ethidium-based probes, Proc. Natl. Acad. Sci. USA 103 (41) (2006) 15038–15043.
[38] E.T. Chouchani, et al., Ischaemic accumulation of succinate controls reperfusion injury through mitochondrial ROS, Nature 515 (7527) (2014) 431–435.
[39] E. Blake, A. Curnow, The hydroxypyridinone iron chelator CP94 can enhance PpIX-induced PDT of cultured human glioma cells, Photochem. Photobiol. 86 (5) (2010) 1154–1160.
[40] A. Pye, S. Campbell, A. Curnow, Enhancement of methyl-aminolevulinate photodynamic therapy by iron chelation with CP94: an in vitro investigation and clinical dose-escalating safety study for the treatment of nodular basal cell carcinoma, J. Cancer Res. Clin. Oncol. 134 (8) (2008) 841–849.
[41] S. Anand, et al., Low-dose methotrexate enhances aminolevulinate-based photodynamic therapy in skin carcinoma cells in vitro and in vivo, Clin. Cancer Res. 15 (10) (2009) 3333–3343.
[42] A. Curnow, S.G. Bown, The role of reperfusion injury in photodynamic therapy with 5-aminolaevulinic acid–a study on normal rat colon, Br. J. Cancer 86 (6) (2002) 989–992.
[43] J. Raffel, et al., Increased expression of thioredoxin-1 in human colorectal cancer is associated with decreased patient survival, J. Lab. Clin. Med. 142 (1) (2003) 46–51.
[44] P.S. Smith-Pearson, et al., Decreasing peroxiredoxin II expression decreases glutathione, alters cell cycle distribution, and sensitizes glioma cells to ionizing radiation and H(2)O(2), Free Radic. Biol. Med. 45 (8) (2008) 1178–1189.
[45] C. Cadenas, et al., Role of thioredoxin reductase 1 and thioredoxin interacting protein in prognosis of breast cancer, Breast Cancer Res. 12 (3) (2010) R44.
[46] J.T. Erler, et al., Hypoxia-mediated down-regulation of Bid and Bax in tumors occurs via hypoxia-inducible factor 1-dependent and -independent mechanisms and contributes to drug resistance, Mol. Cell. Biol. 24 (7) (2004) 2875–2889.
[47] Y.L. Liu, et al., Regulation of ferrochelatase gene expression by hypoxia, Life Sci. 75 (17) (2004) 2035–2043.
[48] H.Y. Cho, et al., Role of NRF2 in protection against hyperoxic lung injury in mice, Am. J. Respir. Cell Mol. Biol. 26 (2) (2002) 175–182.
[49] K.C. Das, X.L. Guo, C.W. White, Hyperoxia induces thioredoxin and thioredoxin reductase gene expression in lungs of premature baboons with respiratory distress and bronchopulmonary dysplasia, Chest 116 (1) (1999) (101s-101s).
[50] P. Carmeliet, et al., Role of HIF-1alpha in hypoxia-mediated apoptosis, cell proliferation and tumour angiogenesis, Nature 394 (6692) (1998) 485–490.
[51] N.S. Chandel, et al., Role of oxidants in NF-kappa B activation and TNF-alpha gene transcription induced by hypoxia and endotoxin, J. Immunol. 165 (2) (2000) 1013–1021.
[52] D.R. Collingridge, et al., Polarographic measurements of oxygen tension in human glioma and surrounding peritumoural brain tissue, Radiother. Oncol. 53 (2) (1999) 127–131.
[53] M. Nordsmark, et al., Measurements of hypoxia using pimonidazole and polarographic oxygen-sensitive electrodes in human cervix carcinomas, Radiother. Oncol. 67 (1) (2003) 35–44.
[54] D.R. Blake, P.G. Winyard, R. Marok, The contribution of hypoxia-reperfusion injury to inflammatory synovitis: the influence of reactive oxygen intermediates on the transcriptional control of inflammation, Ann. N.Y. Acad. Sci. 723 (1994) 308–317.
[55] M.H. Theus, et al., In vitro hypoxic preconditioning of embryonic stem cells as a strategy of promoting cell survival and functional benefits after transplantation into the ischemic rat brain, Exp. Neurol. 210 (2) (2008) 656–670.
[56] K. Ghori, et al., The effect of midazolam on cerebral endothelial (P-selectin and ICAM-1) adhesion molecule expression during hypoxia-reperfusion injury in vitro, Eur. J. Anaesthesiol. 25 (3) (2008) 206–210.
[57] A.M. McCord, et al., Physiologic oxygen concentration enhances the stem-like properties of CD133+ human glioblastoma cells in vitro, Mol. Cancer Res. 7 (4) (2009) 489–497.
[58] T.S. Li, E. Marban, Physiological levels of reactive oxygen species are required to maintain genomic stability in stem cells, Stem Cells 28 (7) (2010) 1178–1185.
[59] D. Futalan, et al., Effect of oxygen levels on the physiology of dendritic cells: implications for adoptive cell therapy, Mol. Med. 17 (9–10) (2011) 910–916.
[60] C.A. Ingraham, et al., Matrix metalloproteinase (MMP)-9 induced by Wnt signaling increases the proliferation and migration of embryonic neural stem cells at low O2 levels, J. Biol. Chem. 286 (20) (2011) 17649–17657.
[61] A. Richter, K.K. Sanford, V.J. Evans, Influence of oxygen and culture media on plating efficiency of some mammalian tissue cells, J. Natl. Cancer Inst. 49 (6) (1972) 1705–1712.
[62] K.S. Sridhar, et al., Effects of physiological oxygen concentration on human tumor colony growth in soft agar, Cancer Res. 43 (10) (1983) 4629–4631.
[63] J.A. Krieger, J.C. Landsiedel, D.A. Lawrence, Differential in vitro effects of physiological and atmospheric oxygen tension on normal human peripheral blood mononuclear cell proliferation, cytokine and immunoglobulin production, Int. J. Immunopharmacol. 18 (10) (1996) 545–552.
[64] Q. Peng, et al., 5-Aminolevulic acid-based PDT: principals and experimental research, Photochem. Photobiol. 65 (2) (1997) 235–251.
[65] J.B. Mitchell, et al., Oxygen dependence of hematoporphyrin derivative-induced photoinactivation of Chinese-hamster cells, Cancer Res. 45 (5) (1985) 2008–2011.
[66] J.D. Chapman, et al., Oxygen dependency of tumor-cell killing invitro by light-activated Photofrin-Ii, Radiat. Res. 126 (1) (1991) 73–79.
[67] B. Diez, et al., Ros production by endogenously generated protoporphyrin IX in murine leukemia cells, Cell Mol. Biol. (Noisy-Le.-Grand.) 55 (2) (2009) 15–19.
[68] Y. Gilaberte, et al., Flow cytometry study of the role of superoxide anion and hydrogen peroxide in cellular photodestruction with 5-aminolevulinic acid-induced protoporphyrin IX, Photodermatol. Photoimmunol. Photomed. 13 (1–2) (1997) 43–49.
[69] H. Xu, et al., Protoporphyrin IX induces a necrotic cell death in human THP-1 macrophages through activation of reactive oxygen species/c-Jun N-terminal protein kinase pathway and opening of mitochondrial permeability transition pore, Cell Physiol. Biochem. 34 (6) (2014) 1835–1848.
[70] H. Zhang, et al., Nrf2-regulated phase II enzymes are induced by chronic ambient nanoparticle exposure in young mice with age-related impairments, Free Radic. Biol. Med. 52 (9) (2012) 2038–2046.
[71] A. Singh, et al., Gain of Nrf2 function in non-small-cell lung cancer cells confers radioresistance, Antioxid. Redox Signal 13 (11) (2010) 1627–1637.
[72] I.S. Song, et al., Mitochondrial peroxiredoxin III is a potential target for cancer therapy, Int. J. Mol. Sci. 12 (10) (2011) 7163–7185.
[73] J. Grim, et al., Low expression of NQO1 predicts pathological complete response to neoadjuvant chemotherapy in breast cancer patients treated with TAC regimen, Folia Biol. 58 (5) (2012) 185–192.
[74] P.G. Winyard, C.J. Moody, C. Jacob, Oxidative activation of antioxidant defence, Trends Biochem. Sci. 30 (8) (2005) 453–461.
[75] S.J. Chapple, et al., Bach1 differentially regulates distinct Nrf2-dependent genes in human venous and coronary artery endothelial cells adapted to physiological oxygen levels, Free Radic. Biol. Med. 92 (2016) 152–162.
[76] B. Haas, et al., Permanent culture of macrophages at physiological oxygen attenuates the antioxidant and immunomodulatory properties of dimethyl fumarate, J. Cell. Physiol. 230 (2015) 10.
[77] D.K. Harrison, P. Vaupel, Heterogeneity in tissue oxygenation: from physiological variability in normal tissues to pathophysiological chaos in malignant tumours, Adv. Exp. Med. Biol. 812 (2014) 25–31.
[78] A. Pastore, et al., Determination of blood total, reduced, and oxidized glutathione in pediatric subjects, Clin. Chem. 47 (8) (2001) 1467–1469.